JOURNAL OF THEORETICAL
AND APPLIED MECHANICS
51, 2, pp. 327-337, Warsaw 2013

INTERACTION BETWEEN MATRIX CRACK AND ELLIPTIC INCLUSION UNDER DYNAMIC LOADINGS

Ying Li, Zhuocheng Ou, Zhuoping Duan, Fenglei Huang
Beijing Institute of Technology, State Key Laboratory of Explosion Science and Technology, Beijing, China
e-mail: zcou@bit.edu.cn

The strain-rate effects on the interaction between a matrix crack and an elliptic inclusion in granule composites under dynamic tensile loadings are investigated numerically. It is found that the crack deflection/penetration behavior depends on the relative strength and local curvature of the interface as well as the loading-rate (or strain-rate). For a certain interfacial strength, there exists a critical strain-rate above which the crack can penetrate across the interface; otherwise, the crack deflection occurs. Moreover, the critical strain-rate is found to be dependent only on the local curvature of the interface near the crack tip regardless of the size and shape of the elliptic inclusions.

Key words: interface, fracture toughness, crack deflection/penetration, granule composites

1. Introduction

The study of interaction between a matrix crack and an inclusion in granule composites such as concrete has been one of the most important and active subjects in the field of interfacial fracture mechanics, which is also the foundation for further research on the micromechanics of dynamic strength and failure of composite materials. Much research work on such an issue has been opened over the past decades (Zak and Williams, 1963; Cook and Erdogan, 1972; Kasano *et al.*, 1986; He and Hutchinson, 1989; Ma and Hour, 1990; Wijeyewickrema *et al.*, 1995; Kolednik *et al.*, 2005; Zhang and Deng, 2007; Xu *et al.*, 2003). For instance, Brara and Klepaczko (2007) investigated experimentally via the Split Hopkinson Press Bar (SHPB) technique the fracture energy of concrete under dynamic tensile loadings and observed that most of the aggregates are ruptured under the loadings with higher loading rates, but remain intact under relatively lower ones. Cotsovos and Pavlović (2008a,b,c) summarized a number of previous experimental data of both the dynamic tension and compression experiments, indicating that the strength of concrete increases with the strain-rate, and, moreover, it seems that there exists a critical strain-rate ($\sim 10^2\,\mathrm{s}^{-1}$) for a certain material above which the strength increasing becomes much faster. Such a break phenomenon of the strength increasing was also observed in other bimaterial systems (Cai *et al.*, 2007; Wei and Hao, 2009). In the opinion of the authors of this paper, the mesoscopic mechanism of such a substantial increase of the dynamic strength across the critical strain-rate should be resulted mainly from the cleavage of the aggregates in concrete, which is closely associated with the crack deflection/penetration behavior under dynamic loadings. That is to say, for an interface with a higher strength, the crack penetrates across the interface and propagates along the self-similar crack growth direction, leading to the so-called "transgranular fracture"; the other one is, for a lower interfacial strength, that the crack will deflect into and propagate along the interface, which results in the so-called "intergranular fracture". Moreover, the apparent material strength can increase intensively by the rupture of the inclusion in composites, because the strength of the inclusion is usually much higher than that of the interface. In fact, Liu *et al.* (2010) carried out a numerical simulation on the strain-rate effects on the deflection/penetration of a crack perpendicular to and terminating at a planar

bimaterial interface under dynamic loadings, and the derived numerical results are basically consistent with the above conjecture.

Promoted by the above considerations and based on the previous investigations, in this study, the influence of the interfacial strength (represented by the relative fracture toughness), the loading-rate (or the strain-rates) and the geometrical features of the inclusion on the interaction between a matrix crack and an elliptic inclusion under dynamic tensile loadings are investigated numerically by using ABAQUS applied software, together with the cohesive zone model. The organization of this paper is as follows. In Section 2, both the numerical finite element and the cohesive zone models are described briefly, and the computational results associated with some discussions are then presented in Section 3. Finally, some conclusions are drawn out in Section 4.

2. Finite element and cohesive zone model

The numerical simulations are carried out under two-dimensional plane strain conditions, and the initial reference coordinate frame is assumed to be the Cartesian coordinate system. The computational domain is depicted in Fig. 1, in which a rectangle matrix ($2L = 20\,\text{mm}$) is embedded with an elliptic inclusion, with an elliptic interface bonded between the matrix and the inclusion, and an edge crack ($l = 9\,\text{mm}$) is located perpendicularly to and terminating at the interface. Both the matrix and the inclusion are assumed to be linear elastic materials, and the zero thickness cohesive elements are inserted along the interface as well as the self-similar crack growth direction inside the inclusion. In addition, the lengths of the elliptic semi-major and semi-minor axis are denoted by a and b, respectively.

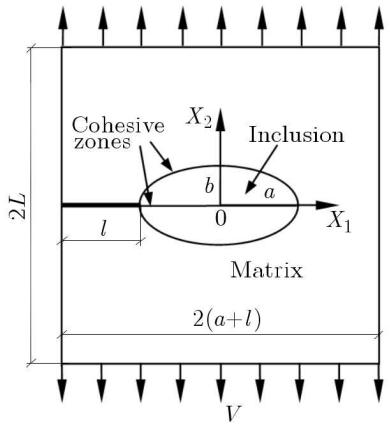

Fig. 1. Computational domain

The velocity boundary conditions acted on the upper and lower boundaries of the computational domain can be written as

$$v(X_1, X_2 = \pm L, t) = \overline{v}(\xi) = \begin{cases} \gamma\xi & \text{for} \quad 0 < \xi \leqslant \xi_r \\ \gamma\xi_r = v_0 & \text{for} \quad \xi > \xi_r \end{cases} \tag{2.1}$$

where v denotes the particle velocity; $\overline{v}$ means the boundary velocity loading; t is the time variable and ξ denotes the local time argument, reckoned from the time when the stress wave arrived at the location under consideration with the loading rising time ξ_r; γ is a constant, which can be used as a measure of the loading rate, and v_0 is the loading amplitude. The material properties of the matrix and the inclusion are presented in Table 1 (Buyukozturk and Hearing, 1998), in which E, ν and ρ represent the Young modulus, the Poisson ratio and the material density, respectively.

Table 1. Material properties

Materials	E [GPa]	ν	ρ [kg/m^3]
Cement	27.8	0.20	1500.0
Aggregate	42.2	0.16	2800.0

In the frame of finite strain continuum, denoting the Lagrangian coordinate and the Eulerian coordinate by $\mathbf{X}$ and $\mathbf{x}$, respectively, the displacement vector $\mathbf{u}$ and the deformation gradient tensor $\mathbf{F}$ are defined, respectively, by

$$\mathbf{u} = \mathbf{x} - \mathbf{X} \qquad \mathbf{F} = \frac{\partial \mathbf{x}}{\partial \mathbf{X}} \tag{2.2}$$

and, in the absence of the body force, the principle of virtual work in the reference configuration, or the governing equations to be solved numerically, can be then written in the following form (Siegmund *et al.*, 1997)

$$\int_V \mathbf{S} : \delta\mathbf{F}\, dV - \int_{S_{int}} \mathbf{T} \cdot \delta\mathbf{u}\, dS = \int_{S_{ext}} \mathbf{T} \cdot \delta\mathbf{u}\, dS - \int_V \rho \frac{\partial^2 \mathbf{u}}{\partial t^2} \cdot \delta\mathbf{u}\, dV \tag{2.3}$$

where $\mathbf{S}$ is the nominal stress tensor; V, S_{ext} and S_{int} are the volume, external and internal surface areas of the considered block, respectively. The traction vector $\mathbf{T}$ on the surface with a normal $\mathbf{n}$ is given by

$$\mathbf{T} = \mathbf{n} \cdot \mathbf{S} \tag{2.4}$$

Two kinds of constitutive relations are used to describe different material behavior in different computational zones. One is the linear elastic Hooke law, which is adopted for both the matrix and the inclusion materials. The other is the cohesive zone model used to describe the interface as well as the self-similar crack growth direction. The cohesive zone model was originally proposed by Barenblatt [19] to eliminate the crack-tip stress singularity in brittle materials, based on which a number of different kinds of cohesive zone models have been developed (Rice and Wang, 1989; Xu and Needleman, 1994; Geubelle and Baylor, 1998; Chandra *et al.*, 2002; Arias *et al.*, 2007) in the field of numerical fracture mechanics. In this study, a bilinear cohesive zone model (Geubelle and Baylor, 1998) is used as given below:

— for $\Delta_n > 0$

$$\begin{aligned} T_n &= \begin{cases} \dfrac{\sigma_{max}}{\Delta_n^*}\Delta_n & \text{for} \quad \Delta_n \leqslant \Delta_n^* \\ \dfrac{\sigma_{max}}{\Delta_{n\,max} - \Delta_n^*}(\Delta_{n\,max} - \Delta_n) & \text{for} \quad \Delta_n^* < \Delta_n \leqslant \Delta_{n\,max} \end{cases} \\ T_t &= \begin{cases} \dfrac{\tau_{max}}{\Delta_t^*}\Delta_t & \text{for} \quad \Delta_t \leqslant \Delta_t^* \\ \dfrac{\tau_{max}}{\Delta_{t\,max} - \Delta_t^*})\Delta_{t\,max} - \Delta_t) & \text{for} \quad \Delta_t^* < \Delta_t \leqslant \Delta_{t\,max} \end{cases} \end{aligned} \tag{2.5}$$

— for $\Delta n = 0$

$$T_t = \begin{cases} \dfrac{\tau_{max}}{\Delta_t^*}\Delta_t & \text{for} \quad \Delta_t \leqslant \Delta_t^* \\ \dfrac{\tau_{max}}{\Delta_{t\,max} - \Delta_t^*}(\Delta_{t\,max} - \Delta_t) & \text{for} \quad \Delta_t^* < \Delta_t \leqslant \Delta_{t\,max} \end{cases} \tag{2.6}$$

where σ_{max} and τ_{max} are the maximum normal and the tangential load-carrying stress of the interface, respectively, which characterizes the initiation of the subsequent material soften process; Δ_n^* and Δ_t^* are, respectively, the normal and the tangential characteristic length parameter

of the interface; $\mathbf{\Delta}$ is the crack open displacement vector, and $\Delta_n = \mathbf{n} \cdot \mathbf{\Delta}$ and $\Delta_t = \mathbf{t} \cdot \mathbf{\Delta}$ are the normal and tangential components of the crack open displacement $\mathbf{\Delta}$, respectively, where $\mathbf{n}$ and $\mathbf{t}$ are the normal and tangential unit vectors of the crack surfaces, respectively, $\Delta_{n\,max}$ and $\Delta_{t\,max}$ represent the critical normal and tangential crack-tip open displacement, respectively, at which complete separation of the two crack surfaces is assumed.

The constitutive relations for Mode I ($\Delta_t = 0$) and Mode II cohesive cracks ($\Delta_n = 0$) are shown in Figs. 2a and 2b, respectively, which describe the relation between the traction acted on the crack surfaces and the crack open displacement. The maximum normal (G_{nc}) and tangential works (G_{tc}) per unit area needed to complete the crack-tip opening (i.e., the total area under the constitutive curve) are given, respectively, by

$$G_{nc} = \frac{\sigma_{max}\Delta_{n\,max}}{2} \qquad G_{tc} = \frac{\tau_{max}\Delta_{t\,max}}{2} \tag{2.7}$$

and the fracture criterion can be written as

$$G_n = G_{nc} \qquad G_t = G_{tc} \tag{2.8}$$

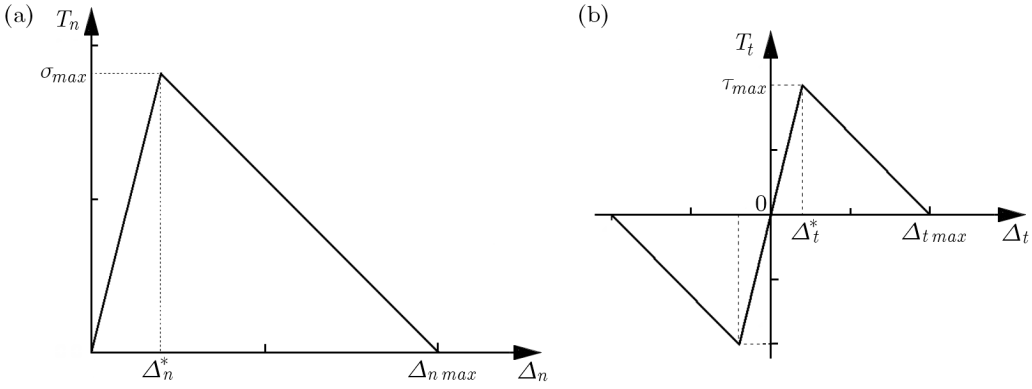

Fig. 2. (a) Cohesive zone model for Mode I crack and (b) for Mode II crack

In the computation, the quadrilateral bulk elements are used as shown in Fig. 3a. At the region ahead of the initial crack, each side of the elements about 20.0 μm in length is used. To save the computation time, the gradual increscent length of meshes out to the region with the length of elements about 20.0 μm is assumed, as shown in Fig. 3b. The zero thickness cohesive elements are inserted into the inclusion along the self-similar crack growth direction as well as the matrix-inclusion interface. The characteristic lengths of the cohesive elements in both

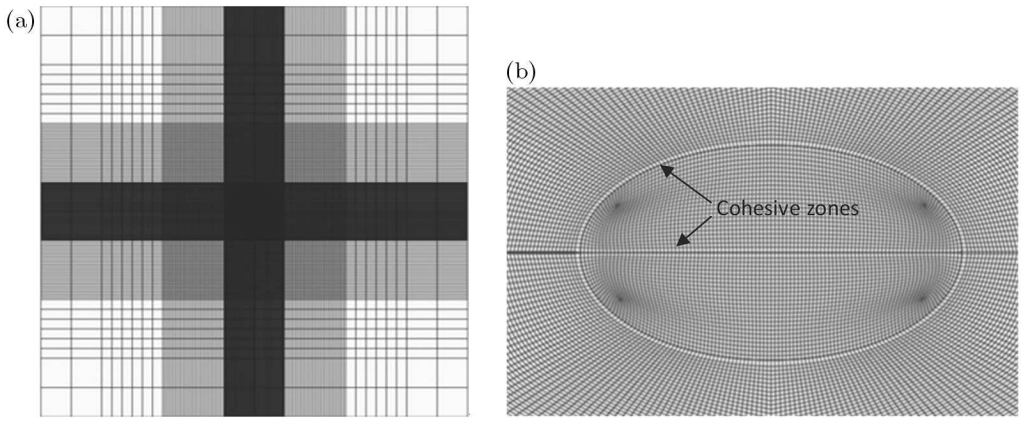

Fig. 3. (a) Finite element meshes; (b) elements near the initial crack-tip

the inclusion and interface are fixed at $\Delta_n^* = \Delta_t^* = 0.1\,\mu$m (Liu *et al.*, 2010), which makes the ratio of length of the element side to the characteristic length about 200 guarantee the computational stability. The constitutive parameters used in the cohesive constitute relation for the inclusion material are taken as $\sigma_{max} = 185.0\,$MPa (Zhang *et al.*, 2005), $\Delta_{n\,max} = 5.4\Delta_n^*$ and $\Delta_{t\,max} = 2.3\Delta_t^*$ (Liu *et al.*, 2010), which results in the maximum normal and shear work needed to complete the crack opening for the inclusion material $G_c = G_{nc} = G_{tc} = 50.1\,\mathrm{J/m^2}$. In addition, it is believed that the computational convergence can be guaranteed when the length of the crack process zone is about five times greater than that of the cohesive elements (Zhang and Paulino, 2005). A simply verification for the availability of the computation can be carried out by using the following equation presented by Rice (1968) to estimate the cohesive zone size

$$l = \frac{\pi}{8}\frac{E}{1-\nu^2}\frac{G_{nc}}{T_{ave}^2} \tag{2.9}$$

where, $T_{ave} = 0.453\sigma_{max}$ (Zhang and Paulino, 2005). It can be easily calculated from Eq. (2.9) that the length of the cohesive zone in the inclusion material is about $l = 121.3\,\mu$m, which can ensure the convergence of the solution (Zhang and Paulino, 2005)]. Moreover, to verify the convergence of the solution, the model with elements having side $15\,\mu$m in length each is also performed. Comparing the results with that of $20\,\mu$m in length shows that basically there is no dependency on the size of finite element meshes.

3. Results and discussion

The effects of the interfacial strength on the crack deflection/penetration behavior under dynamic loadings with certain loading-rates (or strain-rates) are studied at first. For convenience, the interfacial strength (or the relative interfacial strength) is represented by the dimensionless ratio of the interfacial fracture toughness to that of the inclusion material $G_c^{(int)}/G_c^{(2)}$, where the superscripts (1), (2) and (*int*) denote the physical variables for the matrix, inclusion and interface, respectively, and the subscript c denotes the critical value. Figures 4a and 4b show, in a schematic form, the maximum principal stresses in the cases of two interfacial strengths ($G_c^{(int)}/G_c^{(2)} = 0.26,\ 0.27$) under a certain strain-rate ($\dot{\varepsilon}^{(1)} = 856.0\,\mathrm{s^{-1}}$). It can be seen that, for a lower strength interface, the crack deflects into and propagates along the interface, while, in contrast, the crack penetrates across the interface and propagates along the self-similar crack growth direction for a higher strength interface. In other words, corresponding to a given loading rate (or strain rate), there exists a critical value of the interfacial strength above which the crack will penetrate through the interface, otherwise, the crack deviates and grows along the interface. Such a crack deflection/penetration behavior was also confirmed analytically by He and Hutchinson (1989) under quasi-static loading conditions. From a physical point of view, a matrix crack in a homogeneous material should propagate along its self-similar growth direction. However, introduction of an interface as a weaker strength direction in some cases can make the energy redistribution, and then, lead to crack deflection and propagation along the interface. In fact, as two extreme situations, one can think that for an interface with vanishing strength, which implies physically complete separation between the matrix and the inclusion, the crack must "propagate" along the interface, while, on the other hand, the crack should penetrate across the interface with infinite strength just because the interface cannot be fractured at all.

Next, for a certain interfacial strength ($G_c^{(int)}/G_c^{(2)} = 0.28$), the maximum principal stresses under dynamic boundary loadings with different loading-rates (or the strain-rates) ($\dot{\varepsilon}^{(1)} = 400.0\,\mathrm{s^{-1}},\ 800.0\,\mathrm{s^{-1}}$) are shown in Figs. 5a and 5b. It can be found that the crack penetrates across the interface and propagates along its self-similar growth direction under higher strain-rate loadings, while, in contrast, the crack will deflect into and propagate along the

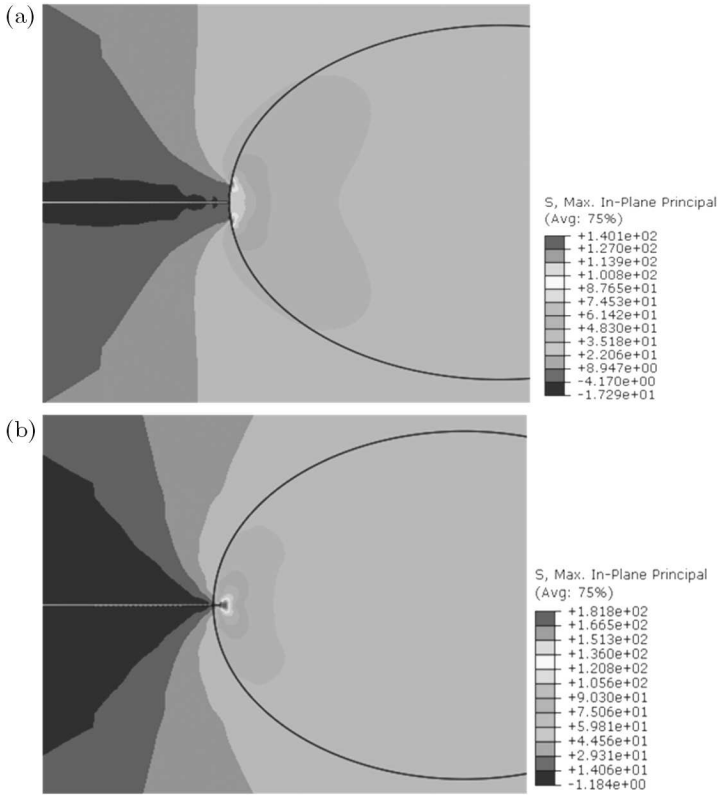

Fig. 4. Contours of maximum principal effective stress and crack location with $\dot{\varepsilon} = 856.0\,\mathrm{s}^{-1}$, $t = 32.0\,\mu\mathrm{s}$; (a) $G_c^{(int)}/G_c^{(2)} = 0.26$, (b) $G_c^{(int)}/G_c^{(2)} = 0.27$

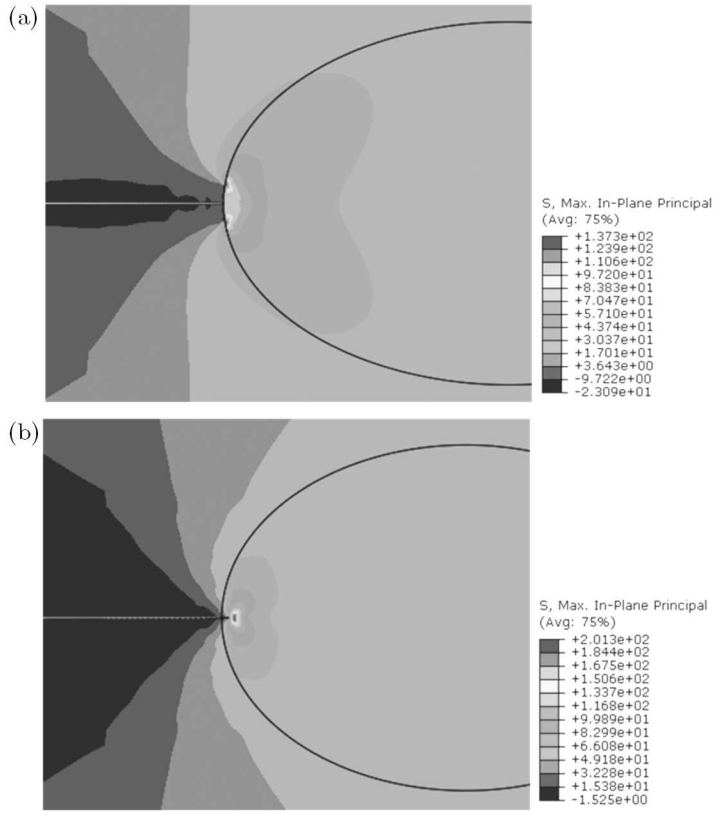

Fig. 5. Contours of maximum principal effective stress and crack location with $G_c^{(int)}/G_c^{(2)} = 0.28$, $t = 32.0\,\mu\mathrm{s}$; (a) $\dot{\varepsilon} = 400.0\,\mathrm{s}^{-1}$, (b) $\dot{\varepsilon} = 800.0\,\mathrm{s}^{-1}$

interface under lower strain-rate ones. In other words, similarly to the existence of the critical interfacial strength, under a certain interfacial strength, there also exists a critical strain-rate, above which the crack penetration and self-similar growth occurs; contrarily, the crack will deflect into the interface. In fact, such dynamic crack deflection/penetration behavior should be attributed to the inertia effects on the energy redistribution. That is to say, under quasistatic or lower strain-rate loadings, when a matrix crack encounters a bimaterial interface, the fracture energy will be redistributed along all the possible directions such as the interface and the self-similar crack growth direction, and the crack will propagate in the direction along which the adopted fracture criterion has been satisfied. However, under the higher strain-rate loadings, there is not enough time for the energy to transfer into the weaker paths because of the material inertia, which makes the crack keep penetrating across the interface and propagating along its self-similar growth direction, although the strength in other direction may be lower. Thus, the higher the strain-rate is, the easier the crack penetration occurs. Moreover, as above mentioned, the failure of the inclusion will dissipate much more energy compared with that of the matrix and the interface because the strength of the inclusion in composites is usually much higher, which leads to a great increasing of the apparent dynamic strength of composites such as concrete. Therefore, the strain-rate effect of material strength under higher strain-rates is significantly stronger than that under a relatively lower strain-rate, which, in fact, has been verified qualitatively by the experimental data on concrete presented by Brara and Klepaczko (2007), in which an increase in the number of fractured aggregates under higher strain-rate loadings was observed. Besides, such a sudden increase of the dynamic material strength over a certain critical strain-rate induced by taking account the inclusion failure is also in agreement with the results presented by Cotsovos and Pavlović (2008b,c). Here, it should be emphasized that all the material parameters used in the computation are quasi-static ones, which implies that the strain-rate effects on material strength are directly dependent on the material inertia as well as the boundary conditions and, thus, are not intrinsic material properties, which has been noticed recently by some investigators (Cotsovos and Pavlović, 2008a,b,c). In other words, the so-called dynamic material strength cannot be considered as a material parameter, which depends on the external loading conditions as well as the inertia properties of the material under consideration.

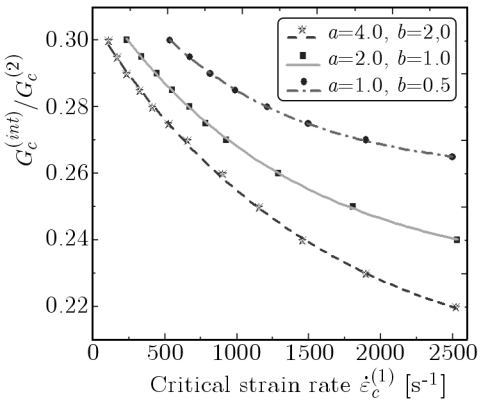

Fig. 6. Relation between the critical strain-rate and the interfacial strength under constant inclusion sizes

Finally, the influence of the inclusion size on the dynamic crack deflection/penetration behavior is investigated. The numerical results for the relation curve between the critical strain-rate and the relative interfacial strength for several given inclusion sizes (a = 4.0, 2.0 and 1.0 mm under $a/b = 2.0$) under a constant crack length $l = 9.0$ mm are presented as shown in Fig. 6. It can be seen, for a certain interfacial strength, the critical strain-rate decreases with the size of the inclusion, which implies that the larger the size of the inclusion is, the easier the crack pene-

tration occurs. Similarly, for a given critical strain rate, the interfacial strength needed to ensure the crack penetration decreases with the inclusion size, which implies that larger inclusions are incident to failure under higher rate dynamic loadings. Moreover, it can be also observed from Fig. 6, as has been described above, that the critical strain-rate decreases monotonously with the interfacial strength. In addition, it should be pointed out, under the similar transformation of the size of the elliptical inclusion by taking the ratio of the semi-major to the semi-minor axis a/b as a constant, both the volume (in three-dimension cases) or the area (in two-dimension cases) of the inclusion and the local curvature of the interface at the crack-tip are different. To explore further the influence of geometrical characteristics of the inclusion on the dynamic crack deflection/penetration behavior, the relationships between the critical strain-rate and both the local curvature of the interface and the area of the inclusion are also investigated in the following. On the one hand, for a constant area of the inclusion ($S = 2\pi \text{mm}^2$), the numerical results for the relation between the critical stain-rate and the interfacial strength under different curvature radii of the interface at the crack-tip, (where $r_c = b^2/a$, and $a = 1.0\,\text{mm}$, $b = 2.0\,\text{mm}$, $a = b = \sqrt{2}\,\text{mm}$ and $a = 2.0\,\text{mm}$, $b = 1.0\,\text{mm}$, respectively) are presented in Fig. 7, which indicate that both the critical strain-rate and the critical interfacial strength decrease with the curvature radius. In other words, the larger the local curvature radius is, the easier the crack

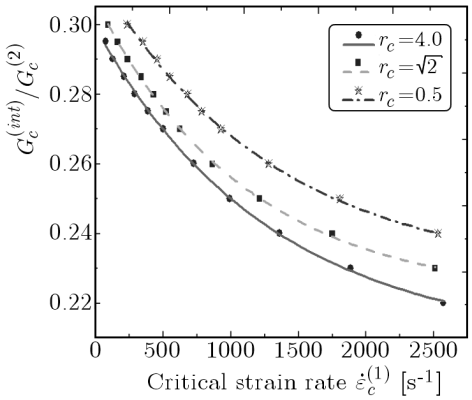

Fig. 7. Relation between the critical strain-rate and the interfacial strength under a constant local curvature of the interface at the crack-tip

penetration occurs, otherwise, the crack deflects into and propagates along the interface. On the other hand, taking a constant local curvature $r_c = 1.0\,\text{mm}$, the numerical results for the relation between the critical strain-rate and the interfacial strength under several given inclusion areas (where $a = 4.0\,\text{mm}$, $b = 2.0\,\text{mm}$, $S = 8\pi\,\text{mm}^2$, $a = 2.0\,\text{mm}$, $b = \sqrt{2}\,\text{mm}$, $S = 2\sqrt{2}\pi\,\text{mm}^2$ and $a = b = 1.0\,\text{mm}$, $S = \pi\,\text{mm}^2$, respectively) are depicted in Fig. 8. It is very interesting to notice that all the computational results under different inclusion areas can be fitted into just one curve with a good precision, and hence a universal relationship may be implied. In other words, the strain-rate effects on the interaction between the matrix crack and the elliptic inclusion under dynamic loadings can be determined by the local curvature of the interface at the crack-tip, independently of the global geometrical properties of the inclusion such as the inclusion size and shape, which will be of important significance in the study of the strain-rate effects on the strength of composite materials. In fact, such a local characteristic is also consistent with the concept of the wave, in which the entire dynamic response can be determined by local properties in the neighborhood near the point under consideration, and the higher the strain-rate, the smaller the neighborhood. From the above description, the influence of inclusion sizes on the strain-rate effects on the dynamic crack deflection/penetration can be then characterized only by that of the local curvature of the interface at the crack-tip. Figure 9 shows, a in schematic form, the numerical results of the local curvature radius as the function of the

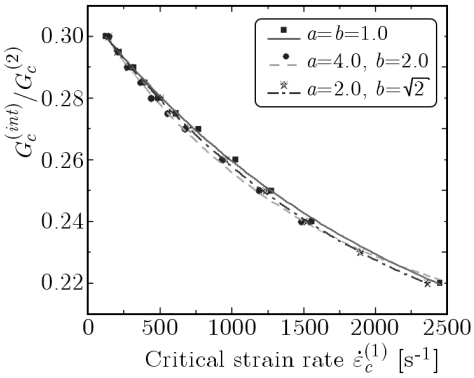

Fig. 8. Relation between the critical strain rate and the interfacial strength under constant inclusion areas

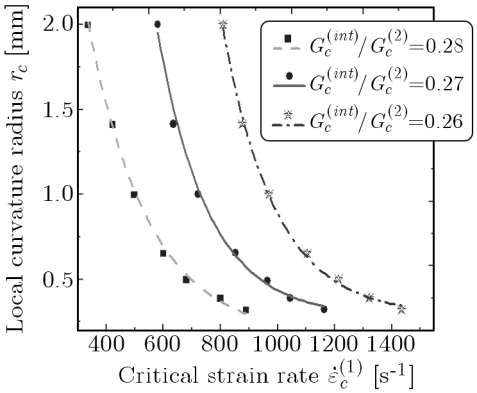

Fig. 9. Rrelation between the critical strain-rate and the local curvature of the interface at the crack-tip under constant interfacial strengths

critical strain-rate under several different interfacial strengths $(G_c^{(int)}/G_c^{(2)} = 0.26,\ 0.27,\ 0.28)$, in which, $a = 2.0\,\text{mm}$ and $b = 0.5,\ 0.8,\ 1.0,\ 1.2,\ \sqrt{2}$ and $2.0\,\text{mm}$, respectively, are assumed.

4. Conclusions

The strain-rate effects on the interaction between a matrix crack and an elliptic inclusion under dynamic loadings are investigated numerically by using ABAQUS applied software, together with the cohesive zone model. It is found from the numerical results that the loading rate (or strain-rates), the relative interfacial strength as well as the local curvature of the interface at the crack-tip can affect extensively the crack deflection/penetration behavior, and some conclusions can be drawn out as follows:

- Under dynamic loadings, the crack deflection/penetration behavior id dependent on the relative interfacial strength. Similarly to the case under quasistatic loadings, for a certain loading-rate (or the strain-rate), there exists a critical value of the relative interfacial strength above which the crack will penetrate across the interface and propagate along its self-similar growth direction. Otherwise, the crack will deflect into and propagate along the interface.
- For a certain relative interfacial strength, the crack can penetrate through the interface only when the strain-rate is higher than the critical strain-rate, which decreases with the interfacial strength, or else the crack will deflect into and propagate along the interface. Furthermore, the strain-rate effects on the dynamic strength of composites can be induced

directly from the structural response of materials because of the inertia effects. Therefore, the strain-rate effects on the dynamic material strength will not be an intrinsic material property, which is consistent with the arguments proposed by Cotsovos and Pavlović 2008a,b,c) and Ou *et al.* (2010).

- Under a given interfacial strength, the critical strain-rate is dependent only on the local curvature of the interface at the crack-tip, regardless of the size and shape of the inclusion, and the critical strain-rate decreases with the local curvature radius of the interface.

Acknowledgements

The paper is supported by the National Science Foundation of China (No. 10872035) and the Foundation of Key State Laboratory of Explosion Science and Technology under contract YBKT09-05.

References

1. Arias I., Knap J., Chalivendra V.B., Hong S., Ortiz M., Rosakis A.J., 2007, Numerical modeling and experimental validation of dynamic fracture events along weak planes, *Computer Methods in Applied Mechanics and Engineering*, **196**, 3833-3840
2. Barenblatt G.J., 1962, The mathematical theory of equilibrium crack in the brittle fracture, *Advance in Applied Mechanics*, **7**, 55-125
3. Brara A., Klepaczko J.R., 2007, Fracture energy of concrete at high loading rates in tension, *International Journal of Impact Engineering*, **34**, 424-435
4. Buyukozturk O., Hearing B., 1998, Crack propagation in concrete composites influenced by interface fracture parameters, *International Journal of Solids and Structures*, **35**, 4055-4066
5. Cai M., Kaiser P.K., Suorineni F., Su K., 2007, A study on the dynamic behavior of the Meuse/Haute-Marne argillite, *Physics and Chemistry of Earth*, **32**, 907-916
6. Chandra N., Li H., Shet C., Ghonem H., 2002, Some issues in the application of cohesive zone models for metal-ceramic interfaces, *International Journal of Solids and Structures*, **39**, 2827-2855
7. Cook T.S., Erdogan F., 1972, Stresses in bonded materials with a crack perpendicular to the interface, *International Journal of Engineering Sciences*, **10**, 677-697
8. Cotsovos D.M., Pavlović M.N., 2008a, Numerical investigation of concrete subjected to high rates of uniaxial tensile loading, *International Journal of Impact Engineering*, **35**, 319-335
9. Cotsovos D.M., Pavlović M.N., 2008b, Numerical investigation of concrete subjected to compressive impact loading. Part 1: A fundamental explanation for the apparent strength gain at high loading rates, *Computers and Structures*, **86**, 145-163
10. Cotsovos D.M., Pavlović M.N., 2008c, Numerical investigation of concrete subjected to compressive impact loading. Part 2: Parametric investigation of factors affecting behaviour at high loading rates, *Computers and Structures*, **86**, 164-180
11. Geubelle P.H., Baylor J., 1998, Impact-induced delamination of laminated composites: a 2D simulation, *Composites Part B-engineering*, **29**, 589-602
12. He M.Y., Hutchinson J.W., 1989, Crack deflection at an interface between dissimilar elastic materials, *International Journal of Solids and Structures*, **25**, 1053-1067
13. Kasano H., Watanabe T., Matsumoto H., Nakahara I., 1986, Singular stress fields at the tips of a crack normal to the bi-material interface of isotropic and anisotropic half planes, *Bulletin of JSME – Japan Society of Mechanical Engineers*, **29**, 4043-4049
14. Kolednik O., Predan J., Shan G.X., Simha N.K., Fischer F.D., 2005, On the fracture behavior of inhomogeneous materials, a case study for elastically inhomogeneous biomaterials, *International Journal of Solids and Structures*, **42**, 605-620

15. Liu L.G., Ou Z.C., Duan Z.P., Huang F.L., 2010, Strain-rate effects on deflection /penetration of crack terminating perpendicular to bimaterial interface under dynamic loadings, *International Journal of Fracture*, **167**, 135-145
16. Ma C.C., Hour B.L., 1990, Antiplane problems in composite anisotropic materials with an inclined crack terminating at a bimaterial interface, *International Journal of Solids and Structures*, **26**, 1387-1400
17. Ou Z.C., Duan Z.P., Huang F.L., 2010, Analytical approach to the strain rate effect on the dynamic tensile strength of brittle materials, *International Journal of Impact Engineering*, **37**, 942-945
18. Rice J.R., 1968, Mathematical analysis in the mechanics of fracture, [In:] Liebowitz H. (Edit.), *Fracture*, **2**, Academic Press, New York
19. Rice J.R., Wang J.S., 1989, Embrittlement of interfaces by solute segregation, *Material Science and Engineering A*, **107**, 23-40
20. Siegmund T., Fleck N.A., Needleman A., 1997, Dynamic crack growth across an interface, *International Journal of Fracture*, **85**, 381-402
21. Wei X.Y., Hao H., 2009, Numerical derivation of homogenized dynamic masonry material properties with strain rate effects, *International Journal of Impact Engineering*, **36**, 522-536
22. Wijeyewickrema A.C., Dundurs J., Keer L.M., 1995, The singular stress field of a crack terminating at a frictional interface between two materials, *Journal of Applied Mechanics*, **62**, 289-293
23. Xu L.R., Huang Y.Y., Rosakis A.J., 2003, Dynamic crack defection and penetration at interfaces in homogeneous materials: experimental studies and model predictions, *Journal of the Mechanics and Physics of Solids*, **51**, 461-486
24. Xu X.P., Needleman A., 1994, Numerical simulations of fast crack growth in brittle solids, *Journal of Mechanics and Physics of Solids*, **42**, 1397-1434
25. Zak A.R., Williams M.L., 1963, Crack point stress singularities at a bi-material interface, *Journal of Applied Mechanics*, **30**, 142-143
26. Zhang M.H., Shim V.P.W., Lu G., Chew C.W., 2005, Resistance of high-strength concrete to projectile impact, *International Journal of Impact Engineering*, **31**, 825-841
27. Zhang W., Deng X., 2007, Elastic fields around the cohesive zone of a mode III crack perpendicular to a bimaterial interface, *ASME Journal of Applied Mechanics*, **74**, 1049-1052
28. Zhang Z.Y., Paulino G.H., 2005, Cohesive zone modeling of dynamic failure in homogeneous and functionally graded materials, *International Journal of Plasticity*, **21**, 1195-1254

Oddziaływanie eliptycznego wtrącenia ze szczeliną w osnowie kompozytu podczas dynamicznego obciążania

Streszczenie

W pracy przedstawiono rezultaty symulacji numerycznych wpływu szybkości zmian stanu naprężenia na interakcje pomiędzy szczeliną w osnowie i eliptycznym wtrąceniu w kompozycie granulkowym poddanym dynamicznemu obciążeniu rozciągającemu. Stwierdzono, że odkształcenie i (lub) penetracja szczeliny zależy od względnej wytrzymałości oraz lokalnej krzywizny powierzchni kontaktu pomiędzy wtrąceniem a osnową. Wykazano także ich zależność od tempa zmian obciążenia (lub odkształcenia). Zauważono, że przy pewnym poziomie wytrzymałości powierzchni kontaktu pojawia się krytyczna wartość tempa zmian odkształcenia, powyżej której szczelina propaguje w poprzek powierzchni kontaktu, w przeciwnym razie ugina się. Zgodnie z wynikami badań, krytyczna wartość szybkości zmian odkształcenia okazała się zależna wyłącznie od miejscowej krzywizny powierzchni kontaktu przy wierzchołku szczeliny, bez względu na rozmiar i kształt eliptycznego wtrącenia.

Manuscript received June 13, 2011; accepted for print April 18, 2012